Int. J. Electrochem. Sci., 12 **(2017)** 6266 – 6281, doi: 10.20964/2017.07.54

International Journal of
ELECTROCHEMICAL
SCIENCE
www.electrochemsci.org

Developing Hybrid–Power Fuel Cells with a Low–Pressure Hydrogen–Storage System used in an Electric Forklifts

Chuang-Yu Hsieh, Xuan-Vien Nguyen, Fang-Bor Weng,Tzu-Wei Kuo, Chi-Yuan Lee, Ay Su[*]

Department of Mechanical Engineering & Fuel Cell Center, Yuan Ze University, Taoyuan 320, Taiwan
[*]E-mail: meaysu@saturn.yzu.edu.tw

Received: 18 October 2016 / *Accepted:* 2 December 2016 / *Published:* 12 June 2017

In this study, we prepared a lab–built water–cooled fuel cell hybrid power system. This system contains 2.7 kW proton exchange membrane fuel cells, ultracapacitors, and lithium batteries that are actually constructed in a commercial electric forklift, APT–20. This hybrid system can conform to the working state of a typical electric forklift, providing lifting loads of 1000 kg at 4 kW. This system is designed to control the fuel cell so as not to exceed its own power generating capacity of 74% in operation, so it is coupled with a fluctuating load of a set of small fuel cells to assist in balancing power. For maximum power output to the lift motor, it is coupled with a set of independent supply lift motors to increase kinetic energy and improve the overall output state. The fuel supply is a low–pressure hydrogen–storage system, consisting of four tanks of low–pressure steel hydrogen–storage cylinders to be used by the fuel cell. It thus provides a safer hydrogen–storage method for use in factory transport vehicles. By designing two sets of auxiliary power sources with different powers, it is anticipated that the fuel cell output can be maintained at 1.8 kW to 2 kW, such that the fuel cell has stable output and prolonged life–span, and can be maintained under a good working environment, and that the overall system has maximum effectiveness in supplying the necessary kinetic energy according to the usage requirements.

Keywords: hybrid power systems, proton exchange membrane fuel cells, lithium–ion battery, ultracapacitor circuits, power management.

1. INTRODUCTION

The proton exchange membrane fuel cell (PEMFC) has the features of quick start–up, zero emissions, high–efficiency energy conversion, etc. [1–4]. Thus, not only can it be used in the construction of power stations, it is also applicable for use as a mobile power source, which is also an ideal choice for electric cars or mobile vehicles.

Since the beginning of the 1920s, the power sources installed in working vehicles have been nothing more than diesel, gasoline, and battery, which are the three main types. Since 2005, however, fuel–cell–powered pallet trucks have been tested in many locations, such as hospitals, warehouses, airports, and other test sites [5]. However, the cost of a fuel cell system is still very high. If hybrid power methods can be adopted, that is, by coupling with lithium batteries and ultracapacitors, such that the fuel cell wattage is reduced and the output energy is stored in different forms, so as to adjust the overall output state of the system, then the weaknesses of a fuel cell system can be improved upon.

To couple a fuel cell system with a power source, there must be an improvement to the power or an auxiliary effect, so a good idea is needed for the design of the coupling. Generally, there are two types of power source configurations: (1) large fuel cell wattage with small auxiliary power wattage and (2) small fuel cell wattage with large auxiliary power wattage. Under general operation, if a fuel cell has small wattage, it is normally used as a back–up power supply or for vehicles that only need a small power source. For use in a factory vehicle, the configuration is not simply decided based on the magnitude of wattage, but can be designed based on the typical use of the factory vehicle. For general use as a factory vehicle, the highest priorities are being able to quickly take a large load and having a short charging time.

There are a few aspects to be considered in the design of a hybrid power system for a factory transport vehicle. (1) Operating mode: An instantaneous response [6–8] is extremely damaging to the membrane–electrode assembly (MEA) at the heart of a fuel cell; an excessive instantaneous tensile load is likely to cause degradation to fuel cell performance. A fuel cell design should prioritize a stable output. (2) Power distribution: A factory vehicle does not use its full power output all the time, but it requires the full power output to be supplied instantaneously. The design needs a short charging or discharging time for power supply. (3) Hydrogen–storage methods: Currently, most studies adopt the conventional metal hydrogen–storage cylinder or high–pressure hydrogen–storage techniques, whereas the direct–methanol fuel cell (DMFC) mainly uses liquid methanol as the main. For a factory vehicle, the cost of a high–pressure steel hydrogen–storage cylinder is low and it is easy to start and assemble. Because under Taiwanese regulations, the pressure of these bottles is capped at 150 psi, the volume must be enlarged for prolonged periods of use. This affects the overall design and structure of factory vehicle, making it larger. Metal hydrogen storage is slightly more expensive and the design is more difficult, but its volume is smaller than that of a high–pressure steel hydrogen–storage cylinder and it can be arranged in accordance with the center of gravity for factory transport vehicles. Both have their pros and cons; if the design is further developed according to the function, then the vehicle can attain the greatest efficiency.

According to current assessments, applying a fuel–cell power system in a factory transport vehicle should be able to reduce the power cost of pure lead–acid batteries by more than 10% [9–11]. The fuel cell power design is coupled with a hybrid power system, which uses both lithium batteries and ultracapacitors as the main components. Lithium batteries have the features of a high energy density, low discharge current, long life–span, etc. [12]. Ultracapacitors have the advantages of rapid charging and discharging, stable output, simple assembly, etc. [13–17]. These features can provide great output as a hybrid power source and can also protect the fuel cell from being damaged by pulse loading. These features make them ideal choices.

This study was designed to conduct practical installation and testing of a lab–built hybrid power system in a factory vehicle; the basic operation and problem solving tasks were undertaken in the laboratory. By utilizing a fuel cell as the main power source, it is anticipated that two coupled sets of auxiliary power sources can be designed in accordance with requirements to not only protect the fuel cell, but also provide a suitable power source.

2. EXPERIMENTAL

2.1. Fuel cell system

This study adopted a lab–built PEMFC stack as a power source. This fuel–cell power generation system was formed by stacking forty sets of fuel cells. For the fuel cell stack, each single unit cell can generate 0.975 V in the open circuit state; when fully loaded, it is approximately 0.65 V. The operating voltage of this cell stack ranges from 39 V to 26 V and the maximum power can be up to 2.7 kW. In the design of the system output, only 60% to 70% of fuel cell's power is required. This range allows the fuel cell to have a stable output and prolongs the fuel cell's life–span. The fuel cell's specifications are as shown in Table 1.

This fuel cell system is shown in Figure 1. The hydrogen gas for the anode was provided by four tanks of low–pressure metal–hydrogen–storage cylinders; the pressure of the hydrogen gas was 7 psi.

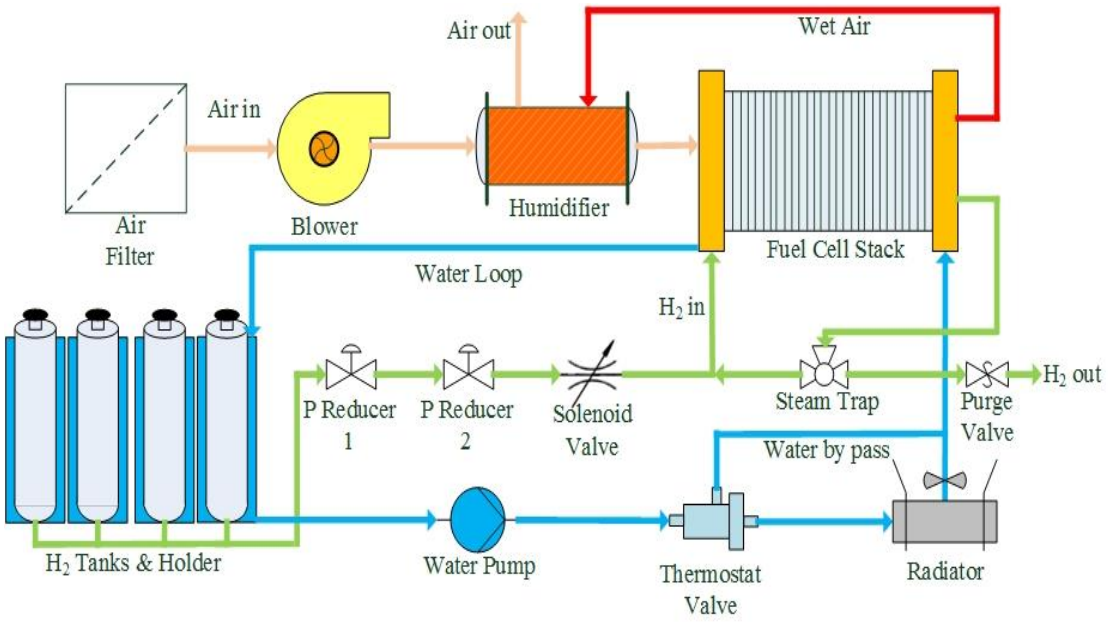

Figure 1. Schematic diagram of the framework of the fuel cell system.

At the cathode terminal, the air was supplied by a blower. Using ambient air, the uncleaned air source was filtered by an air filter installed at the front end and then the air entered the humidifier.

After the humidified air entered the fuel cell and completed the reaction, the wet air was discharged through the outlet of the humidifier outlet. The water cooling system was controlled by a water pump through a thermostatic valve, so that water at 55 °C entered the main body of the fuel cell stack to control the temperature. As the metal–hydrogen–storage cylinder provided hydrogen gas and generated an endothermic reaction, the low temperature caused a problem of being unable to supply the hydrogen gas. After passing through the fuel cell, cooling water with higher temperature can provide the metal–hydrogen–storage cylinders with sufficient heat to restore the operating temperature, so the cooling water outlet of the fuel cell is connected to the cooling water jacket of the metal–hydrogen–storage cylinder and then the water is returned to the water pump. This circulation can resolve an excessively high water temperature in the fuel cell and it is an appropriate scheme for the metal–hydrogen–storage cylinders that require a heating system. The detailed specifications of the hybrid–power fuel cell system are as shown in Table 1.

Table 1. Parts of the fuel cell system.

Name	Specifications
PEMFC stack	40 cells, 150 cm^2
Low–pressure steel–hydrogen–storage cylinder	HSC-500-L
Water jacket of hydrogen–storage tank	HSC-500-WJ
Quick coupling of hydrogen-storage tank	HSC-500-QC
Thermostat valve for water circulation	BOP-01-001 Operating temperature: 40–45 °C Port diameter: 13 mm
Water pump for circulation	BOP-02-001 Max flow rate: 10 L/min Operation voltage: 24 VDC Power: 28 W
Water radiator & fan	BOP-03-001 BOP-04-001

2.2. Low-pressure metal-hydrogen-storage tanks

Hydrogen gas was stored in the tanks containing the metal hydride powder $LaNi_5H_6$ (called the AB alloy). This is currently recognized as the safest hydrogen–storage method. The operating temperature ranged from 25 °C to 120 °C and hydrogen desorption occurred at pressures below 10 psi, which is very suitable for the operating temperature of a fuel cell. This hydrogen–storage process has the physical characteristics of exothermic hydrogen adsorption and endothermic hydrogen desorption, and thus the waste heat of the fuel cell can heat up the metal hydrogen–storage cylinder via water circulation. Using a water jacket can not only transfer the heat to the hydrogen–storage cylinder for use, but also eliminate the need for a radiator device, which reduces the complexity of the system. This method is the same as for cooling of an internal combustion engine, but the heat transfer mechanism is different. Finally, when replacing the metal cylinders, connectors equipped for quick

connecting/disconnecting can be easily changed [18–21]. Specifications of the low–pressure metal–hydrogen–storage cylinders are shown in Table 2.

Table 2. Specifications of the low-pressure metal-hydrogen-storage cylinders.

Item	Specification
Main body material	6061-T6 aluminum alloy
Dimensions	Length 365 mm × diameter 76 mm
Hydrogen–storage material	AB5
Inflation pressure	140 psi
Hydrogen desorption pressure	<10 psi
Capacity	>45 g/tank @8.0Slpm, 50 °C
Weight	4.5 ± 0.1 kg/tank

2.3. Hybrid power system

This hybrid power system was designed for the chosen model of electric forklift. A diagram of the set–up is shown in Figure 2 [17]. Standard specifications are shown in Table 3. The required power for the travelling motor was 1.8 kW at 24 V and the required power for the lifting motor was 2.5 W at 24 V. The settings can be divided into the modes of (1) traveling and (2) lifting.

(1) Travelling mode of Part A: Taking the fuel cell stack operating at 1.6–2 kW at 26 V as the main source of the power supply, the auxiliary power system is composed of a 24 V/20 Ah lithium battery and 23-F ultracapacitors in parallel. After the fuel cell and the auxiliary power supply are in parallel, the power is converted via a DC/DC converter to supply power to the travelling motor being used. The output power has a fixed voltage of 29 V; the auxiliary contacts of the magnetic contactor are used to conduct the control loop for charging the auxiliary power system of Part B. (2) Lifting mode of Part B: When a load is applied on the lifting side, the magnetic contactor jumps onto the charging mode, Part B begins to discharge power on the lifting motor, and the DC/DC converter output terminal no longer charges Part B. Once the lifting motor stops moving, the magnetic contactor immediately jumps back to the charging mode and the output terminal of the DC/DC converter begins charging Part B again. Since the DC/DC converter's output voltage is fixed at 29 V, the auxiliary power of Part B will not be discharged to the traveling motor.

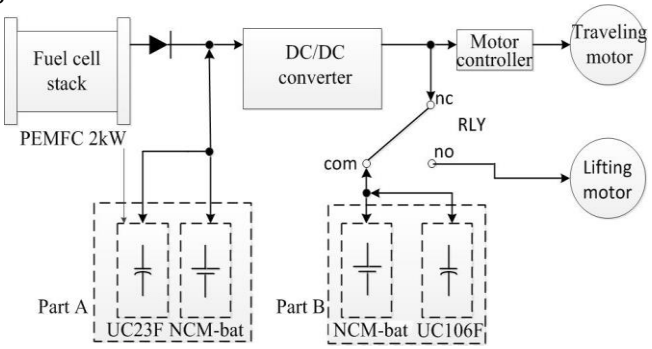

Figure 2. Diagram of the hybrid system set–up.

Table 3. Specifications of the hybrid power system

Project	Specification
Part A	
Lithium battery	VISTA Advance Tech @ NCM–peak 24V / 20Ah / 7S2P
Ultracapacitors	13 ultracapacitors in series, a string 35.1 V/ 23 F
Part B	
Lithium battery	VISTA Advance Tech @ NCM–peak 24V / 20Ah / 7S2P
Ultracapacitors	12 ultracapacitors in series, 4 parallel group 32.4 V / 106 F

2.4. Circuit configuration of the electric forklift

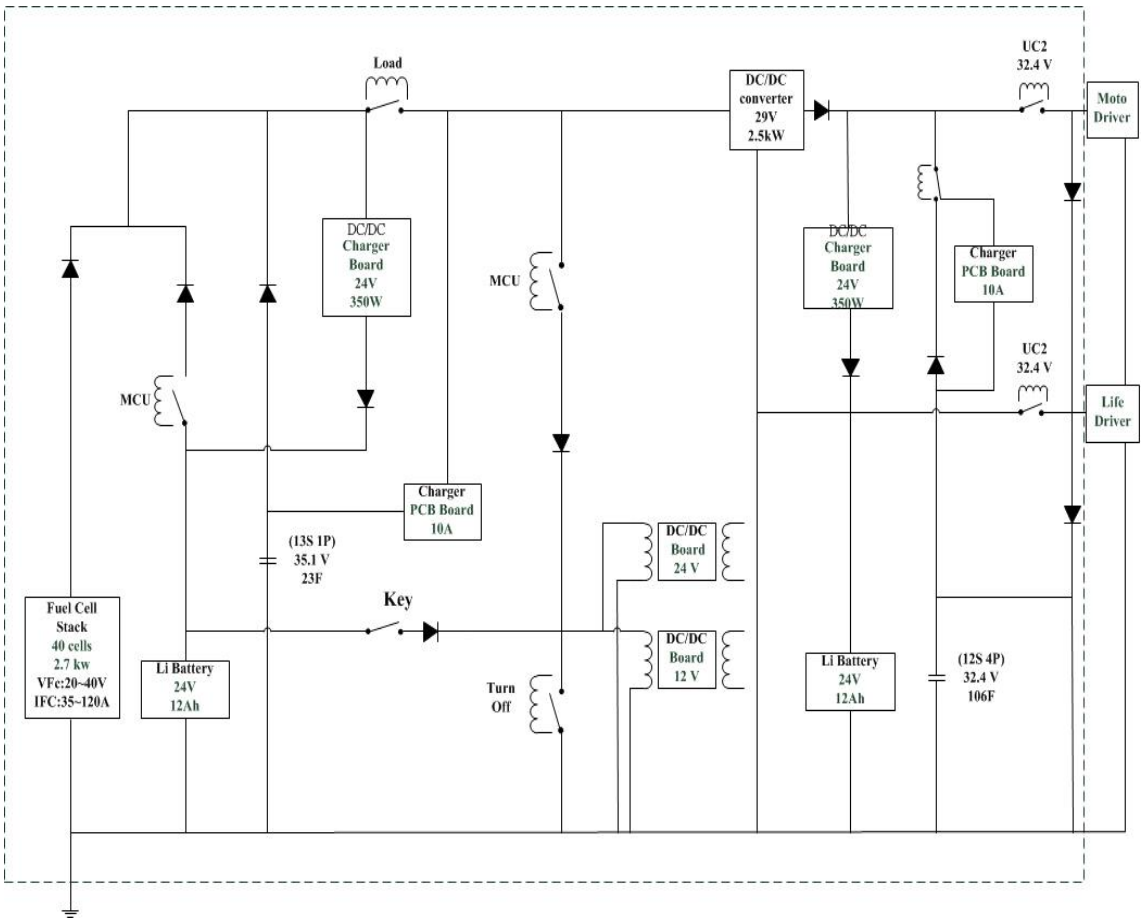

Figure 3. Circuit diagram of the ternary power sources in an electric forklift.

The circuit design is the overall central of an electric forklift. The power management distributions are illustrated in Figure 3. The hybrid system with ternary power sources was connected

to the DC/DC converter in order to preliminarily stabilize the voltage and current. A ternary hybrid power system is connected to the Schottky diodes for power distribution. This arrangement achieves the maximum output supplied by the fuel cell under an ideal standby state. The fuel cell in its operating state has a maximum current limit of 120 A and a minimum voltage of 20 V for the largest fuel cell. This limitation mainly takes accounts for fuel cells that are not capable of larger fluctuating loads and need to be maintained at a voltage of 0.6 V for each sub–cell, in order to preserve the life–span of the fuel cell system. The lacking portion will be assisted by both the modules of the lithium battery and ultracapacitors.

2.5. Hybrid system logic compilers

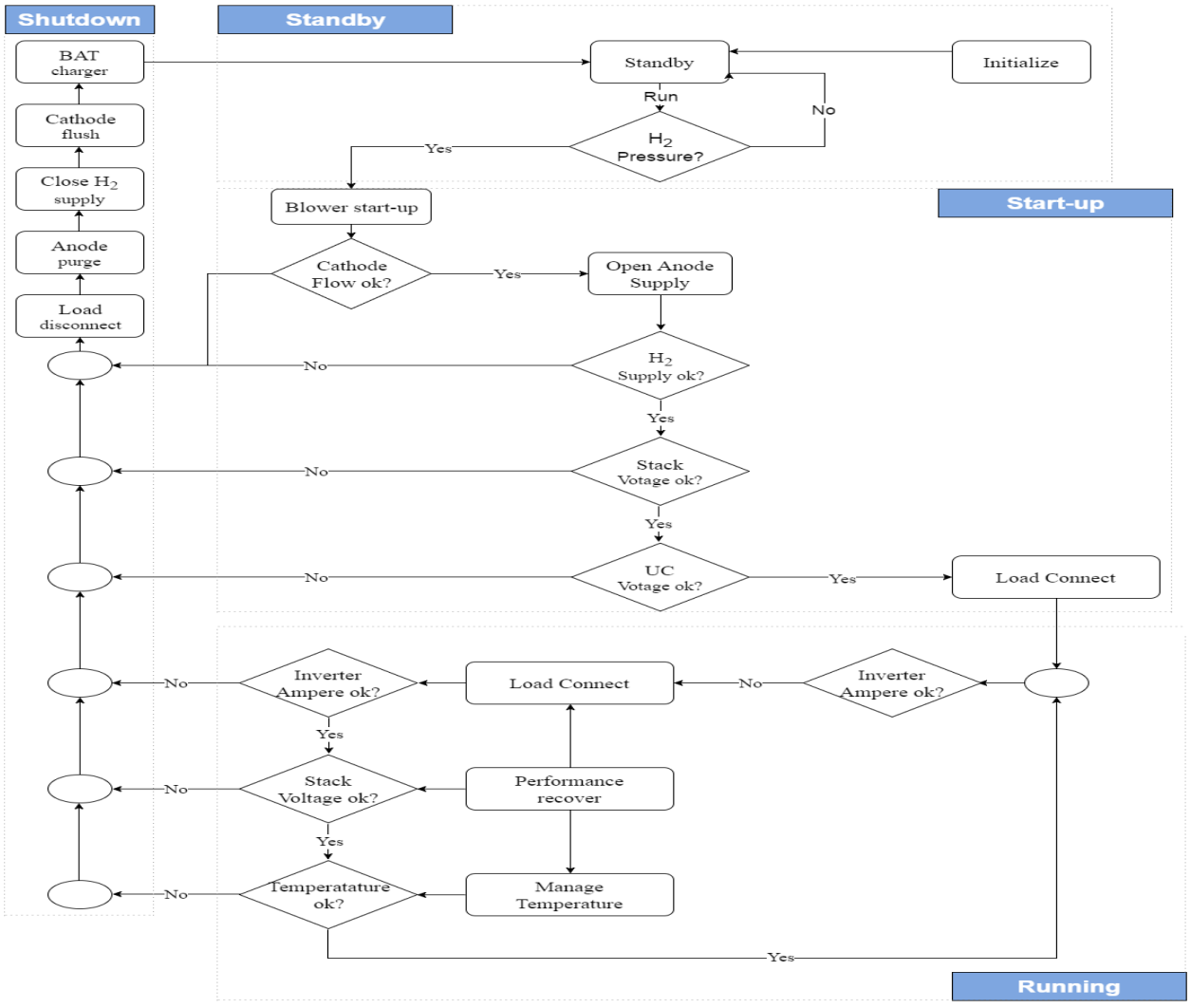

Figure 4. Simplified flowchart of the control program.

The hybrid system design uses a micro–integrated–circuit control unit (MCU) and the processor uses a senary mode unit, and scans every 200 milliseconds for system monitoring and management of all aspects. It simultaneously carries out the data processing of each sensor unit by

sending a signal instantly to the control unit to achieve its goals. In this segment, management is required for the logic compiler. The system needs to have intact programs to manage the control loops. In this study, a set of programmed logic compiler diagrams is configured for the fuel cell system, as shown in Figure 4.

The logic compilers can be divided into four parts:

1. Standby program: By turning on the switch via a key, this action triggers the system to maintain a standby state. Booting the system requires an external power source to supply electricity to the MCU, so that the analytic components can be started up. The initial source of the power supply comes from the lithium battery, and the MCU starts working to detect whether the hydrogen–gas supply terminal has sufficient pressure to provide gas, as the triggering condition for the next program.

2. Start–up program: To provide an adequate preparation scheme for the fuel cell system corresponding to the load of the electric pallet truck, the blower is started up to provide the cathode–side air supply and the humidifier is initialized. In normal operation, the solenoid valve actuator for the anode side is turned on to supply hydrogen gas, and simultaneously a reciprocating pump is used to maintain the normal supply of hydrogen in the pipeline. By this point in time, the fuel cell has gradually achieved the ideal state. In coordination with the circulation of cooling water, the power of the fuel cell stack tends to be stable. Finally, it is necessary to detect if the supercapacitors have sufficient power. The objective of the booting start–up state is achieved, relays of continuous loads will be open and connected, and the controller components of the electric pallet truck combine the hybrid power system and can conduct load operations.

3. Running program: Being divided into the twin aims of travelling and lifting, this experiment primarily focuses on travel–end processing and the protection of the fuel cell by maintaining normal output power via the output of the converter. If an excessive current is detected, the system will immediately measure whether the supply for the transport end, the voltage of the cell stack, and the temperature of the cooling system are processing normally. If there is any item not meeting the conditions, then the program will switch immediately to shutdown program processing.

4. Shutdown program: When encountering situations that do not meet the conditions, the system will immediately run the shutdown program. The program first disconnects the continuous relay at the load side, the system's electricity will be switched to the control side of the electric pallet truck, and the solenoid valve will be turned off, before the residual hydrogen supply in the cell stack undergoes a purging action. At the anode end, the airflow of the blower is increased to maintain clean fresh air, and the residual electricity in the cell stack and capacitor module is returned to charge the lithium battery, in order to maintain optimum energy recovery until the end, and it is restored to the original standby stage. In order to avoid accidents, this phase protects system safety and flow performance.

2.6. Mechanical framework for the electric forklift system

In the design of the mechanical framework for an electric forklift, Taiwan is one of the few nations that specifically provide fuel cell designs for pallet trucks. Therefore, we purchased a model

with lead–acid batteries from manufacturers and then made modifications. The vehicle body used is an APT–20 from Noveltek Industrial Manufacturing Inc., Taiwan. The appearance and specifications are respectively shown in Table 4.

Table 4. Specifications of the electric forklift.

Specifications	**ATP-20**
Load capacity	2000 kg
Load center	600 mm
Lifting speed	Not loaded: 1.5 s Fully loaded: 2.0 s
Lowering speed	Not loaded: 2.5 s Fully loaded: 2.5 s
Adjustable travel speed and output power of motor	
Travel speed	Not loaded: 6.0 km/h Fully loaded: 5.5 km/h
Gradeability	Not loaded: 18% Fully loaded: 8%
Vehicle weight	480 kg

The space originally designed for the placement of the lead-acid battery was re–designed to accommodate the multiple hybrid systems. A three–dimensional layout was first designed for the mechanical framework. Designing to suit a limited space can simulate implementation problems, avoid wasting time, and increase operating speed.

During the operation process, we take into consideration the problems of collision or vibration, so it is necessary to assign the positions of components during placement. After the arrangement test, it was found that the fuel cell system requires more space, so it is placed at the lower level. The lithium battery is placed in the upper layer for ease of replacement and measurement. The ultracapacitor module can be placed in a scattered arrangement and connected with load lines.

3. RESULTS AND DISCUSSION

3.1. Fuel cell performance curves

Of the three hybrid power sources, the fuel cell is the overall main power source. Good or bad fuel cell performance will thus affect the source of main driving force and the charging capability. Therefore, it has an absolute relationship to how well a fuel cell can function within the overall system. As indicated by Figure 5, the best operating conditions for the fuel cell stack are a hydrogen equivalence of 1.4, an air equivalence of 3.0, and an operating temperature of 55 °C. The fuel cell stack can generate 2.7 kW, but if the fuel cell is used for prolonged periods of time at extreme efficacy, the fuel cell will age rapidly. In view of the experimental data, if the fuel cell is operated at a range of 0.65 V (40 cells, 26 V), then the rate of aging will be effectively reduced. Therefore, the operating conditions are set to the lowest value voltage at 26 V; the minimum voltage to protect against power failure is 20 V. These results are compared with those of previous studies. Two PEM fuel cell stacks

with a nominal electric power of 1.5 kW (each), which have been designed, fabricated and assembled, are used to power the vehicle. Each of them consists of 60 cells delivering a nominal voltage in the range 24–30V [22]. A light electric vehicle (golf cart, 5 kW nominal motor power) was integrated with a commercial 1.2 kW PEM fuel cell system. The system results in the extension of the vehicle driving range by 63–110%, when the amount of the stored H_2 fuel varies within 55–100% of the maximum capacity (0.28kg H_2) [23]. The integrated fuel cell system into a lightweight vehicle was presented by Hwang et al. [24]. The fuel cell system consisted of a 3.2 kW PEMFC, the vehicle performed satisfactorily over a 100 km drive on a plain route with the average speed about 18 km/h. Measurements showed that the fuel cell system had an efficiency of over 30% at the power consumption required for vehicle cruise, which is higher than that of a typical Internal Combustion Engine.

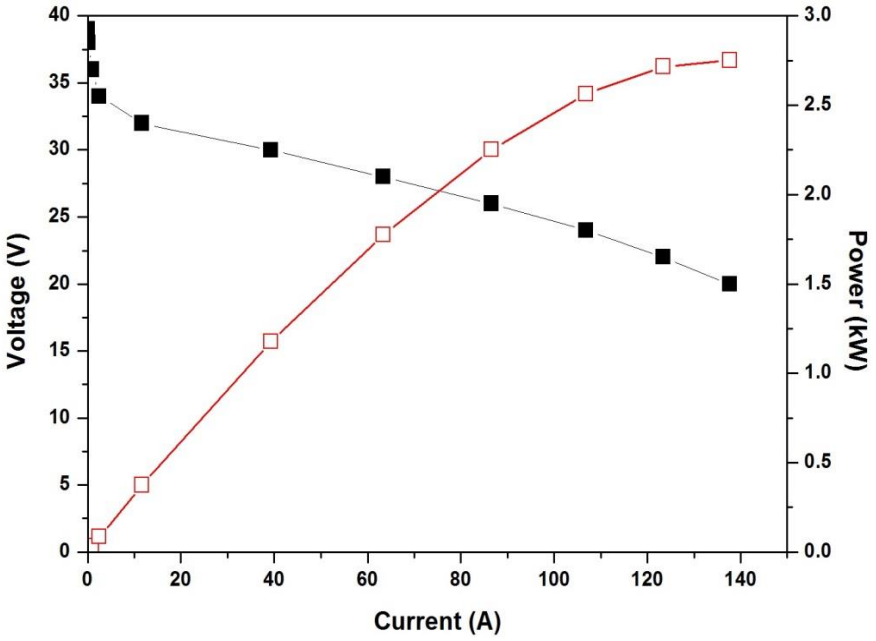

Figure 5. Fuel cell performance curves.

3.2. Operation of the fuel cell system

For the fuel cell system placed on board the electric forklift, the temperature of the fuel cell is essential to achieving the full performance. The cooling method used for a kilowatt–scale fuel cell is water cooling, so the mechanism by which water dissipates heat is critical. The temperatures measured by the cycle tests of the three modes of traveling, slope–climbing, and lifting in the experiment are shown in Figure 6(a). In the graph, the fuel cell temperatures fall within 55–60 °C; the water temperature was around 45 °C. The measured temperature of the fuel cell does not vary much with the operating conditions. This can be attributed to the low–pressure hydrogen–storage tanks. As the discharge of hydrogen from the low–pressure hydrogen–storage tank requires energy and while there is waste heat from the fuel cell, this heat–exchange design can meet these conditions and reduce the burden on the cooling system. When the fuel cell system is operated under a high power state, if the

performance of a single cell is too low, then it will affect the operating life–span and the aging speed of the fuel cell system. Keränen et al. [7] showed the control of the cooling system was realized with the PEMFC coolant outflow's temperature rate of change. The operation temperature was kept mostly between 53 °C and 56 °C in the laboratory system and between 50 °C and 55 °C in the forklift power source. This is 10 °C lower than the maximum operation temperature specified by the stack manufacturer, but was chosen due to the low recirculation rate of the anode fuel. Besides, they also showed the voltage of every single unit cell falls approximately in the range of 0.60 V to 0.63 V. As shown in Figure 6(b), the measurements of the fuel cells under an operating state of 26 V, and the voltage of every single unit cell falls approximately in the range of 0.64 V to 0.66 V. As indicated, the lab–built fuel cell system in the assembly does not have many flaws, so it can be used in a transport vehicle and permit successful operation.

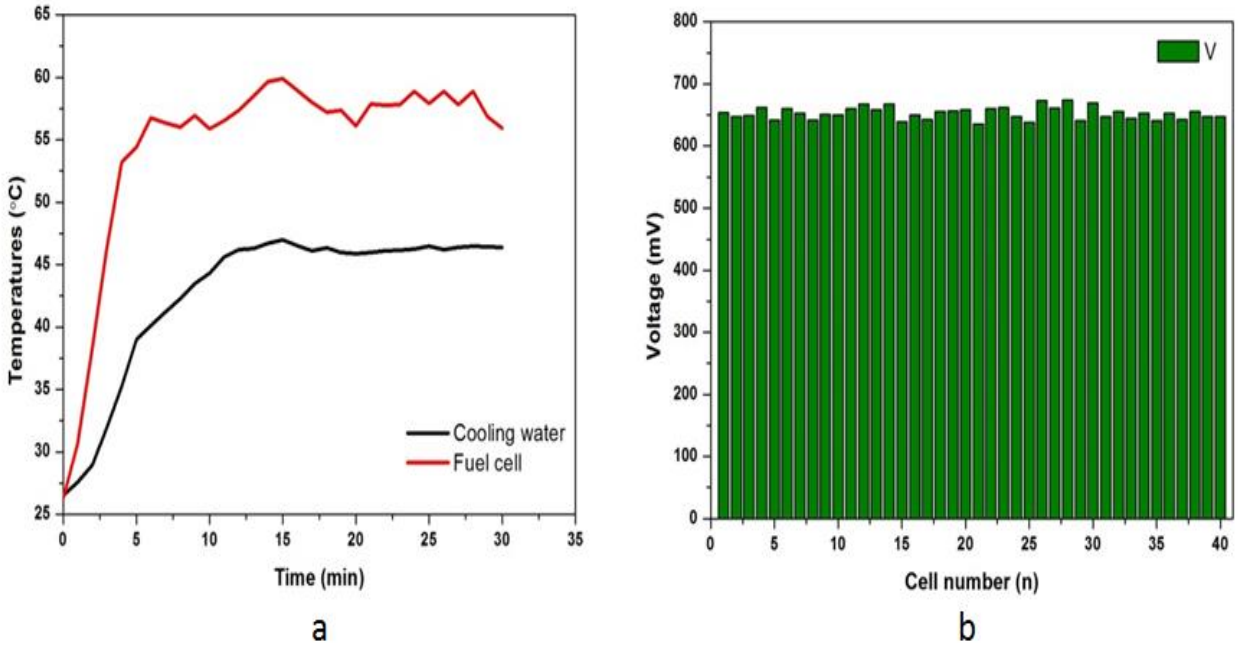

Figure 6. (a) Operating temperatures of the system and (b) voltage distribution of single cell at fuel cell operating voltage of 26 V.

3.3. Test operation of a fuel cell forklift with ternary power sources

3.3.1. Traveling model

In this experiment, the entire system was placed on a pallet truck to test its operation. For the test methods, three modes were planned: traveling, slope–climbing, and lifting weights. Figure 7 shows the operation of the pallet truck in a general traveling state. When the start–up process of the traveling motor needs to resist maximum friction in order to travel, it requires greater energy to drive it. In order to enable a smooth electrochemical reaction in the fuel cell and increase the power, the initial state is aided by the auxiliary power of Part A (lithium battery and ultracapacitors) to provide power; the instantaneous auxiliary power was 2 kW. When the fuel cell system can provide a state with a power

of 1.8 kW, the auxiliary power of Part A will be disconnected and the power will be mainly supplied by the fuel cell stack for traveling at a speed of 6 kph. If the fuel cells are operating under an instantaneous response as normal, this will cause rapid aging, so the auxiliary power of Part A mitigates the problem of instantaneous response by the fuel cell. Chen et al. [25] investigated the dynamic response of each power source to the variation of load power. The overall stack performance measured in this study is lower than that provided by its manufacturer. The main reason is that in this study the supplied hydrogen was not humidified, resulting in lower membrane conductivity. Wu et al. [26] shows the dynamic response of the fuel cell–supercapacitor passive hybrid to a 100 A pulse load from no–load conditions. Upon application of the step load, the supercapacitors initially handled all the load, as the thermodynamic OCP of both devices was the same under steady state conditions.

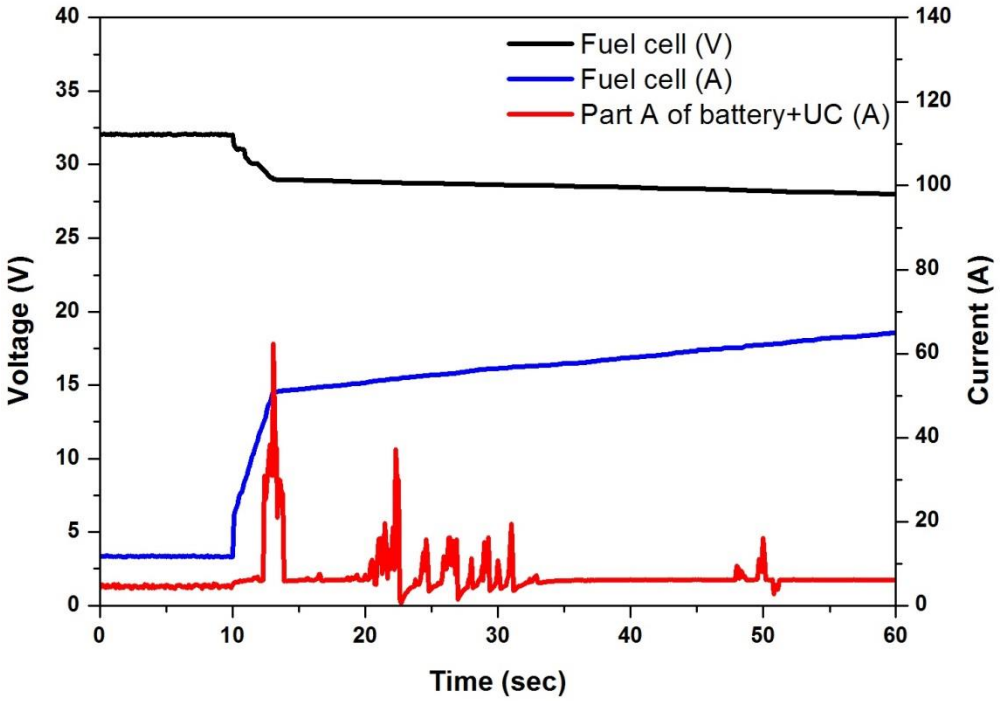

Figure 7. Traveling performance of a fuel cell forklift with ternary hybrid drive system.

3.3.2. Slope–climbing mode

When entering the state for climbing a slope, the average power required is 3.6 kW. Using the discharge characteristics of a 5C lithium battery, coupled with the output of the fuel cell, the power can meet the requirements for climbing the slope. As shown in Figure 8, the system is in a traveling state in time interval of 70 s to 78 s. The joint outputs from the fuel cell and the auxiliary power and the power distribution trends are the same as in Figure 7. After 78 sec, the pallet truck moved on to a road surface with a climbing slope, the current of the fuel cell increased moderately, and the auxiliary current of Part A supplied up to 100 A. With a stable output of 2 kW from the fuel cell, the auxiliary power source supplied 2.1 kW of power to make up for the insufficient power. The experiment showed that the voltage output of the fuel cell was stable without drastic changes. This design can thus

satisfy the slope–climbing conditions. Based on this power distribution, the pallet truck can support goods with a load of 1 ton and climb a 7° slope at a speed of 5 kph. The Fuel Cell current or power slope must be limited to avoid the fuel starvation problem. Normally, the Fuel Cell limited current or power slope has been experimentally determined as the highest slope of operated fuel cell system, where no fuel starvation occurs, for example, $4As^{-1}$ for a 0.5-kW, 12.5-V PEMFC [27]; and a $2.5kWs^{-1}$ for a 40-kW, 70-V PEMFC [28]. Supercapacitor is the highest dynamic power source, which provides the micro-cycles and the fast dynamic power supply. Battery is between FC and supercapacitor in the dynamic classification.

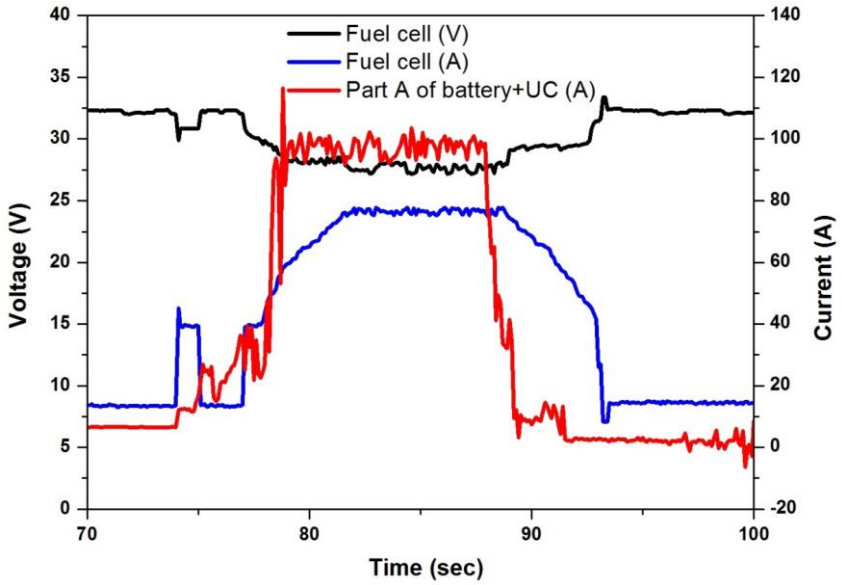

Figure 8. Slope–climbing performance of a fuel cell forklift with ternary hybrid power system.

3.3.3. Lifting mode

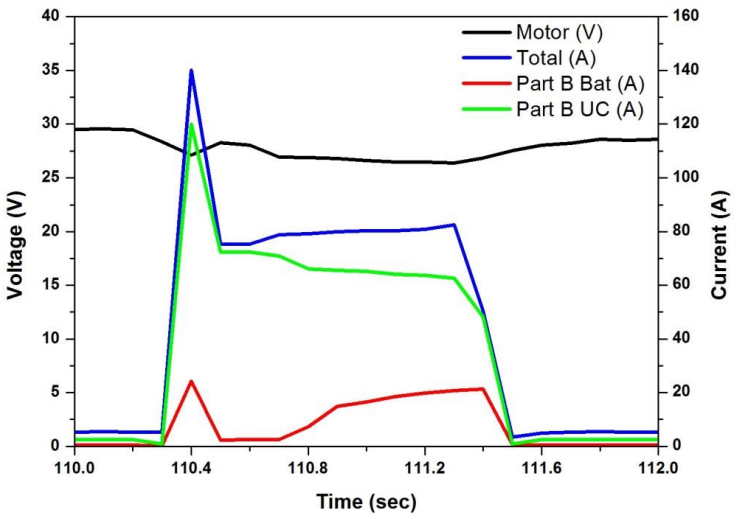

Figure 9. Lifting performance of the fuel cell forklift with ternary hybrid power system.

The lifting state requires an instant power output and the lifting takes approximately 1.5 seconds to raise the fork and carried goods to the maximum height. The instant power was 3.8 kW and the time taken was 0.2 s. If simply using the fuel cells coupled with the auxiliary power of Part A, then an output of only 2.1 kW can be delivered. There is obviously insufficient power. The design in Part B independently supplies power for the use of lifting and it can instantly reach the requirement of 3.8 kW. When the lifting motor was starting up, the ultracapacitors in Part B could instantly provide 125 A, which was approximately 3.3 kW. The voltage of the ultracapacitors dropped to 28 V after discharging the current load. Because the ultracapacitors and lithium battery are in parallel, the lithium battery will discharge simultaneously. The lithium battery provided a current of 25 A, which was approximately 600 W. This parallel state could provide an instant power of 3.8 kW within 0.2 s. The subsequent power was 2.5 kW; the time taken was 1.1 s. The voltage of the lifting motor continued to drop. This indicates that the voltage of the ultracapacitors also continued to drop, and the lithium battery could then easily make up for lacking parts, as shown in Figure 9. Electric forklifts (Classes I, II, and III) come in a variety of lift capacities, from 3000 lb to 20,000 lb, although most electric forklifts are in the 3000 lb to 6000 lb range [29]. Vural et al. [15] carried out using a test bench, which employs a PEMFC (5 kW, 48 V), and a storage device composed of two different types of UC banks (165 F-48 V and 430 F-16 V) corroborate the performances of both applied energy management strategies during similar motor drive cycles. During motor starts/stops or other significant steps in load, the storage elements provide the balance of energy needed during the momentary load transition period; and also absorbs excess energy from regenerative braking. Thounthong et al. [30] presented simulation results during a high constant stepped load power. There are the load, supercapacitor, battery, and fuel cell power. In simulation, the FC minimum and maximum powers are set at 0.0pu and 1.0pu, respectively, and the battery minimum and maximum powers are set at −0.2pu (corresponding to the maximum charging current) and 1.0pu (corresponding to the maximum discharging current), respectively.

4. CONCLUSIONS

This study had the following outcomes:

1. The hybrid system on the test machine was successfully transplanted onto a transport vehicle, and the actual lifting weight was 1 ton. It can indeed withstand the workload of transporting typical heavy objects in a warehouse.

2. By dividing the auxiliary power sources into two sets to be configured according to different outputs, the full characteristics of the lithium batteries and ultracapacitors can be utilized and the fuel cells can maintain normal operation. In the future, the auxiliary power source can be changed in accordance with the requirements, saving the need and the cost for purchasing large–scale fuel cells.

3. In the traveling and slope–climbing modes, aided by the lithium battery and ultracapacitors, the fuel cell in the instant start–up process can resolve the problem of an instant tensile load. After the test, it was found the auxiliary power source of Part A could complete the task as an auxiliary power source and protect the fuel cells.

4. In an experimental test, the auxiliary power of Part B fully supplied 3.8 kW for the task of lifting 1 ton of heavy objects in 0.2 s. As demonstrated by the experimental test, the power provided by the auxiliary system of Part B is indeed sufficient for the lifting mode. In addition, by reducing the power and usage life–span of a fuel cell, as well as reducing the costs, it indeed fully utilized the discharge characteristics of the lithium battery and supercapacitors.

ACKNOWLEDGEMENT
The authors gratefully acknowledge the financial support from the Taiwan Asia-Pacific Fuel Cells program (contract FCS–W–150–036) and the Fuel Cell Center, Yuan Ze University.

References

1. San Martin JI, Zamora I, San Martin JJ, Aperribay V, Torres E and Eguia P., *Energy*, 35 (2010) 1898.
2. Carton JG and Olabi AG, *Energy*, 35 (2010) 4536.
3. Park Sehkyu and Popov Branko N., *Fuel*, 88 (2009) 2068.
4. Therdthianwong Apichai, Saenwiset Pornrumpa and Therdthianwong Supaporn, *Fuel*, 91 (2012) 192.
5. Vicki P. McConnell, *Fuel Cells Bulletin*, 2010 (2010) 12.
6. Haroune Aouzellag, Kaci Ghedamsi and Djamel Aouzellag, *Int. J. of Hydrogen Energy*, 40 (2015) 7204.
7. T.M. Keränen, H. Karimäki, J. Viitakangas, J. Vallet, J. Ihonen, P. Hyötylä, H. Uusalo and T. Tingelöf, *J. Power Sources*, 196 (2011) 9058.
8. Hassan Fathabadi, *Energy Conversion and Management*, 103 (2015) 573.
9. J. Kurtz, K. Wipke, S. Sprik, T. Ramsden, C. Ainscough and G. Saur, Spring 2011 composite data products ARRA material handling equipment (ODE), Technical report, Department of Energy, U.S., 2011.
10. Todd Ramsden, An evaluation of the total cost of ownership of fuel cell-powered material handling equipment (ODE), Technical report, Department of Energy, U.S., 2013.
11. Tomás Larriba, Raquel Garde and Massimo Santarelli, *Int. J. of Hydrogen Energy*, 38 (2013) 2009.
12. Andrzej Lewandowski and Maciej Galinski, *J. Power Sources*, 173 (2007) 822.
13. O.A. Ahmed and J.A.M Bleijs, *Renewable and Sustainable Energy Reviews*, 42 (2015) 609.
14. Qi Li, Weirong Chen, Zhixiang Liu, Ming Li and Lei Ma, *J. Power Sources*, 279 (2015) 267.
15. B. Vural, A.R. Boynuegri, I. Nakir, O. Erdinc, A. Balikci, M. Uzunoglu, H. Gorgun and S. Dusmez, *Int. J. Hydrogen Energy*, 35 (2010) 11161.
16. M.C. Kisacikoglu, M. Uzunoglu and M.S. Alam, *Int. J. Hydrogen Energy*, 34 (2009) 1497.
17. Chuang-Yu Hsieh, Xuan-Vien Nguyen, Chang-Tsair Chang, Fang-Bor Weng,Tzu-Wei Kuo, Zhen-Ming Huang and Ay Su, *Int. J. Electrochem. Sci.*, 11 (2016) 10449.
18. Jenn Jiang Hwang and Wei Ru Chang, *J. Power Sources*, 207 (2012) 111.
19. Jenn Jiang Hwang and Wei Ru Chang, *Int. J. Hydrogen Energy*, 35 (2010) 11947.
20. Jenn Jiang Hwang, *Renewable and Sustainable Energy Reviews*, 12 (2012) 3803.
21. Jenn Jiang Hwang, *Renewable and Sustainable Energy Reviews*, 14 (2010) 1390.
22. Felix Barreras, Mario Maza, Antonio Lozano, Sergio Bascones, Vicente Roda, Jose E. Barranco, Manuel Cerqueira and Arturo Verges, *Int. J. Hydrogen Energy*, 37 (2012) 15367.
23. Ivan Tolj, Mykhaylo V. Lototskyy, Moegamat Wafeeq Davids, Sivakumar Pasupathi, Gerhard Swart and Bruno G. Pollet, *Int. J. Hydrogen Energy*, 38 (2013) 10630.
24. Hwang JJ, Wang DY and Shih NC, *J. Power Sources*, 141(2005) 108.

25. Yong-Song Chen, Sheng-Miao Lin and Boe-Shong Hong, *Energies*, 6 (2013) 6413.
26. Billy Wu, Michael A. Parkes, Vladimir Yufit, Luca De Benedetti, Sven Veismann, Christian Wirsching and et al., *Int. J. Hydrogen Energy*, 39 (2014) 7885.
27. Phatiphat Thounthong, Stephane Raël and Bernard Davat, *J. Power Sources*, 158 (2006) 806.
28. P. Rodatz, G. Paganelli, A. Sciarretta and L. Guzzella, *Control Eng. Pract.*, 13 (2005) 41.
29. Amgad Elgowainy, Linda Gaines and Michael Wang, *Int. J. Hydrogen Energy*, 34 (2009) 3557.
30. Phatiphat Thounthong, Stephane Raël and Bernard Davat, *J. Power Sources*, 193 (2009) 376.